The shaping of planetary nebula Sh 2-188 through interaction with the interstellar medium

C. J. Wareing[1]*, T. J. O'Brien[1], Albert A. Zijlstra[2], K. B. Kwitter[3], J. Irwin[4],
N. Wright[5], R. Greimel[6] and J. E. Drew[7]

[1] *Jodrell Bank Observatory, University of Manchester, Macclesfield, Cheshire, SK11 9DL, UK*
[2] *School of Physics and Astronomy, University of Manchester, Oxford Road, Manchester, M13 9PL, UK*
[3] *Department of Astronomy, Williams College, 33 Lab Campus Drive, Williamstown, MA 01267, USA*
[4] *Institute of Astronomy, Cambridge University, Madingley Road, Cambridge, CB3 0HA, UK*
[5] *University College London, Department of Physics & Astronomy, Gower Street, London, WC1E 6BT, UK*
[6] *Isaac Newton Group of Telescopes, Apartado de corras 321, E-38700 Santa Cruz de La Palma, Tenerife, Spain*
[7] *Imperial College of Science, Technology and Medicine, Blackett Laboratory, Prince Consort Road, London, SW7 2BW, UK*

ABSTRACT

Sh 2-188 is an example of strong interaction between a planetary nebula (PN) and the interstellar medium (ISM). It shows a single arc-like structure, consisting of several filaments, which is postulated to be the result of motion through the ISM. We present new Hα images from the Isaac Newton Telescope Photometric Hα Survey of the Northern Galactic Plane (IPHAS) which reveal structure behind the filamentary limb. A faint, thin arc is seen opposite the bright limb, in combination forming a closed ring. Behind the faint arc a long wide tail is detected, doubling the size of the nebula. The nebula extends 15 arcmin on the sky in total. We have developed a 'triple-wind' hydrodynamical model, comprising of the initial 'slow' asymptotic giant branch (AGB) wind and the later 'fast' stellar wind (the interacting stellar wind model), plus a third wind reflecting the motion through the ISM. Simulations at various velocities of the central star relative to the ISM indicate that a high velocity of 125 km s^{-1} is required to reproduce the observed structure. We find that the bright limb and the tail already formed during the AGB phase, prior to the formation of the PN. The closure of the ring arises from the slow–fast wind interaction. Most of the mass lost on the AGB has been swept downstream, providing a potential explanation of the missing mass problem in PNe. We report a proper motion for the central star of 30 ± 10 mas yr^{-1} in the direction of the bright limb. Assuming the central star is moving at 125 ± 25 km s^{-1}, the distance to the nebula is estimated to be 850^{+500}_{-420} pc, consistent with a spectroscopic distance to the star. Expansion velocities measured from spectroscopic data of the bright filaments are consistent with velocities measured from the simulation. Sh 2-188 is one of the largest PNe known, with an extent of 2.8 pc. The model shows that this size was already set during the AGB phase.

Key words: hydrodynamics – planetary nebulae: individual: Sh 2-188, S188, Simeiz 22 – stars: AGB and post-AGB – ISM: structure – stars: mass-loss.

1 INTRODUCTION

The accepted theory of planetary nebula (PN) formation is the interacting stellar winds model (ISW) (Kwok 1982; Balick 1987) where a fast wind ($\sim 10^3$ km s^{-1}) from the hot central star of a PN blows into the slow wind (~ 10 km s^{-1}) produced during the preceding asymptotic giant

branch (AGB) phase. The inner regions of the slow wind are compressed into a dense shell and ionised by the energetic UV radiation of the central star. The familiar ring-like appearance of PNe is then observed. Structures in the nebula are normally attributed to asymmetries in the slow wind, related to physical properties of the central star, such as rotation or binarity.

Observations of PNe have shown several cases where the outer shell shows the only departure from symmetry.

---

* E-mail: cwareing@jb.man.ac.uk

For those cases, the cause of the asymmetries has been proposed to be an interaction with the interstellar medium (ISM). Interaction of PNe with the ISM was first discussed by Gurzadyan (1969). An early theoretical study by Smith (1976) assumed a thin shell approximation and the 'snow-plough' model of Oort (1951). Isaacmann (1979) used the same approximation with higher velocities and ISM densities. Both of these studies concluded similarly that a nebula fades away before any disruption of the nebular shell becomes noticeable.

In contrast, Borkowski et al. (1990) found that many PNe with large angular extent show signs of PN–ISM interaction, and that all nebulae containing central stars with a proper motion greater than 0.015 arcsec yr^{-1} do so. Soker et al. (1991) hydrodynamically modelled the interaction. The PN shell is first compressed in the direction of motion and then in later stages this part of the shell is significantly decelerated with respect to the central star. Both conclude that the interaction with the ISM becomes dominant when the density of the nebular shell drops below a certain critical limit, of typically $n_H = 40 \text{cm}^{-3}$ for a PN in the Galactic Plane.

Villaver et al. (2003) (hereafter referred to as VGM) pointed out the PN–ISM interaction had only been studied by considering the relative movement when the nebular shell had already formed. They performed 2D hydrodynamic simulations following the full AGB phase followed by the PN phase (Vassiliadis & Wood 1993, 1994), with a conservative relative velocity of the central star of 20 km s^{-1} and conservative conditions of the surrounding ISM of $n_H = 0.1 \text{cm}^{-3}$. VGM concluded that interaction provides an adequate mechanism to explain the high rate of observed asymmetries in the external shells of PNe. Further, they conclude that stripping of mass downstream during the AGB phase provides a possible solution to the problem of missing mass in PN whereby only a small fraction of the mass ejected during the AGB phase is inferred to be present during the post-AGB phase. Observational evidence for the effect of the ISM on AGB wind stuctures was found by Zijlstra & Weinberger (2002).

The PN Sh 2-188 (Sharpless 1959) is among the most extreme examples of ISM interaction. The nebula has a one-sided (semi-circular), filamentary appearance. It is a large nebula, with a reported 340 arcsec diameter (Acker et al. 1992); the currrent paper shows it to be considerably larger. It is located in the Galactic plane at $l = 128°$, $b = -4°$. New data are presented showing the faint back of the shell and an extended Hα tail. The unusual appearance suggests a high proper motion and makes Sh 2-188 an important test case for PN–ISM interaction at high velocity. We have developed a 'triple-wind' model using a initial slow AGB wind, a subsequent fast post-AGB (PN) wind, and adding a third wind reflecting the movement through the ISM into the ISW model. We use a hydrodynamic scheme developed by Wareing (2005), to investigate whether this triple-wind model can reproduce the nebular shape of Sh 2-188 without requiring magnetic fields. We support the results of the model with a proper motion study of the candidate central star.

Table 1. Estimates of the distance to, radius of and age of Sh 2-188.

| D | R | t | Source |
pc	pc	kyrs	
600	0.5	12.1	Napiwotzki & Schoenberner (1995)
800 ± 300		26.0	Saurer (1995)
965^{+1000}_{-600}	0.88	22	Napiwotzki (1999, 2001)

2   OBSERVATIONS

2.1   Sh 2-188

Sh 2-188 (PNG 128.0−04.1, also known as Simeiz 22) was photographed in 1965 by Gaze & Shain (1965). Spectroscopic work (Parker 1964; Lozinskaya & Esipov 1971; Johnson 1975; Kwitter 1979) revealed the object to have an extremely high [NII] $\lambda6583$ / Hα $\lambda6563$ line-ratio. Further spectroscopic data on the filamentary structure (Rosado & Kwitter 1982) indicated filament densities of a few hundred H cm^{-3} and found abundances similar to Peimbert Type I PN, where the large over-abundances of He and N result from CNO enrichment of the stellar envelope prior to shell ejection (Peimbert 1981). Mapping at radio wavelengths (Israel & Felli 1976; Salter et al. 1984) found only a weak source which appeared to have a flat (thermal) spectrum. This observational evidence, along with the relatively bright optical appearance and PN abundances, constituted a convincing argument to classify the object as a PN, rather than a supernova remnant where non-thermal radio emission would be expected.

Kwitter et al. (1988) identified the candidate central star of the nebula with geometric, colour and apparent magnitude methods. The star is displaced from the geometric centre of the nebula. They estimate a percentage probability of finding an unrelated blue star in the nebula to be 1-2 per cent at most. In their spectroscopic investigation of central stars of old PNe, Napiwotzki & Schoenberner (1995) classified the candidate central star as hydrogen-rich. Borkowski et al. (1990) suggested that the filaments are most probably thin, sheetlike layers of shock-compressed nebular gas, parallel to the line of sight. The majority of the filaments are aligned along the crescent-shaped outer rim, but they noted a few appear to be along the nebular symmetry axis, possibly indicating stellar motion in that direction, as similar filaments do in Abell 35.

Table 1 shows various recent estimates of the distance and physical parameters of the nebula. Various historical estimates can be found in table 5 of Saurer (1995). We do not list statistical distances (e.g. Cahn et al. 1992): the Shklovski method (constant PN mass) particularly is of too low accuracy. Saurer (1995) calculated an extinction distance based on published UBV photometry of stars in the angular vicinity used to construct a reddening distance relationship for the line of sight towards the nebula. Most recently, the NLTE modelling method of Napiwotzki (1999, 2001) has implied the nebula is ancient with the central star at the turning point before the UV flux switches off and the star enters the white dwarf cooling regime. The pa-

Figure 1. An image of Sh 2-188 created by a mosaic of images taken as part of the IPHAS survey in 2003 (see text). The faint central star is approximately 0.5 arcmin East of the brightest star in the centre of the nebula. North is up and East to the left. The image is 9.0×8.5 arcmin.
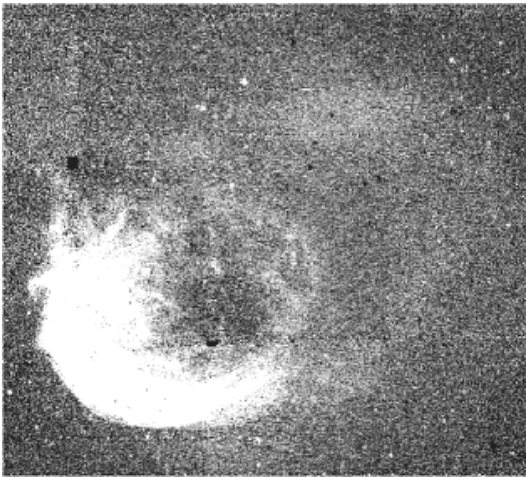

Figure 2. Same as Fig. 1 but with scaling chosen to reveal faint structure. North is up and East to the left. The image shows a faint ring completing the bright semi-circular arc and tails stretching away connecting in the north-west. The ring is centred approximately at RA = 1^h 30^m 25^s, Dec = $+58°$ $25'$ $30''$ (J2000). The image is 18.0×17.0 arcmin.

rameters of Sh 2-188 are still subject to large uncertainties. Consistently though, this nebula is found to be an evolved object and as such is included in the Atlas of Ancient PNe (Tweedy & Kwitter 1996).

Tweedy & Kwitter (1996) note the existence of faint structure to the north-west of the bright nebula. They favour a simple explanation that the gas in this direction has diffused away. They infer a highly inhomogeneous ISM to the south-east producing the bright filaments but essentially absent to the north-west. A more likely model is one of a high peculiar velocity through a uniform ISM, and this is explored below.

2.2 Hα observations

Fig. 1 shows an image of Sh 2-188 created by a mosaic of new Hα $\lambda 6563$ observations taken as part of the Isaac Newton Telescope Photometric Hα Survey of the Northern Galactic Plane (IPHAS) (Drew et al. 2005). The IPHAS survey entails wide-field imaging through Hα, r′ and i′-band filters. It uses the Wide-Field Camera (WFC) at the 2.5-m INT, located at La Palma. The goal of the survey is to image the entire northern Galactic plane between $-5°$ and $+5°$, to study emission-line stars and nebulae. The WFC consists of four 4k×2k CCDs, in an L-shape configuration. The pixel scale is 0.33 arcsec and the instantaneous field is about 0.3 square degrees. Exposure times are 120 s for Hα and 10 s for i′ and r′ for the observations presented here. Each pointing is supplemented by a second one offset by 5 arcmin SW, to cover the gaps between the CCDs. The pointings together provide a tiled pattern that minimizes the gaps, but because of the L-shape CCD configuration small gaps do appear.

The area around Sh 2-188 was observed on 2003 Oct 13 and 14. The seeing varied between 1 and 1.5 arcsec. The airmass was between 1.2 and 1.4. Data reduction was done using the pipeline procedures, which correct for the bias, flat-fielding, non-linearity and geometric distortions. A detailed description can be found in Drew et al. (2005). Fields around the position of Sh 2-188 were retrieved and mosaiced together using the Virtual Observatory software package MONTAGE. The pixel scale was binned to 1 arcsec. A $40'$ field was mosaiced. The r′ was subtracted from the Hα image to bring out the faint emission in this crowded field. MONTAGE tends to leave gradients across the full field, an artifact of the process of background matching of fields taken with different sky brightness. This linear gradient was subtracted.

The final image in Fig. 1 shows the bright portion of the nebula in the south-east, which describes a semi-circular arc with a diameter of 10 arcmin. Due to seeing variations between the r′ and Hα frames, small core-halo residuals can be seen at the positions of bright stars. Stars can also leave positive or negative residuals due to the stellar absorption features in the Hα and/or r′ filter. The bright residual star just behind the brightest part of the shell is an M5 giant, where the r′ filter covers a TiO absorption band. We stress that this is not an emission-line star, nor is it the central star of the PN. The central star of the PN is approximately 0.5 arcmin East of this star. Negative residuals tend to identify stars with strong Hα absorption. The rectangular hole is one of the gaps left by the tiling pattern.

IPHAS provides both images and a source catalogue, as described in Drew et al. (2005). The catalogue contains stars and small resolved objects but not large scale nebulosities. Coordinates are derived by globally matching the stellar sources with all-sky astrometric catalogues. The internal precision is within 0.1 arcsec, and agreement with external catalogues is 0.25 arcsec (e.g. USNO) to 0.1 arcsec (2MASS). We will use the IPHAS source catalogue below in the discussion on the proper motion of the central star.

Structure first noted by Tweedy & Kwitter (1996) to the north-west of the nebula is now revealed by these observations to be a faint circular closure of the bright nebula with connecting tails stretching behind. Fig. 2 has scaling chosen to reveal this structure. From the front of the fila-

mentary structure to the connecting tails the nebula is 15 arcmin long. The surface brightness of the tail is less than 1 per cent of that of the bright filaments. The tail seems to be stretching away from the nebula in opposition to an inferred direction of motion which could explain the one-sided brightening as an interaction with the ISM.

Fig. 3 shows an artificial combination of two three-colour images of the field. One is scaled to show detail in the bright filamentary structure and the other to show the faint structure. The r′ and the i′ bands are coded as blue and green respectively, while Hα is coded as both red and yellow. The central star is indicated and is clearly displaced towards the bright arc from the geometric centre of the nebula.

3   THE TRIPLE-WIND MODEL

A hydrodynamical code has been used to simulate the interaction with the ISM. The numerical scheme used to solve the hydrodynamics equations uses the second-order Godunov scheme due to Falle (1991). The scheme is in 3D cartesian coordinates, fully parallel and includes the effect of radiative cooling (Wareing 2005).

The numerical domain consists of a cubic grid with 200 cells in each direction and uniform cell spacing. The central mass-losing star is placed at cell coordinates $(50, 100, 100)$ and the simulation is performed in the frame of reference of the star. Mass loss is effected by means of setting the values of density, momentum and energy density in the cells in a spherical region of radius $5\frac{3}{4}$ cells centred on the star. The radius of the source volume has been chosen by an experimental process whereby it is a balance between producing the most spherical nebula when modelling the stationary ISW model with spherically symmetric winds (i.e. reducing the pixelation of the cartesian grid) and not being large enough to interfere with the results of the simulation. The conditions within this region are reset at the beginning of every timestep to keep driving the wind. Movement through the ISM is parallel to the x-axis and material flows in at the $(x = 1)$ boundary with a positive x-velocity. All other boundaries have conditions allowing material to flow out of the domain freely.

The hydrodynamic variables in the source volume are set according to the ISW model of the PN–ISM interaction. This follows the evolution of the AGB and post-AGB phases from the beginning of the AGB phase through the post-AGB or PN phase. In the triple-wind model, this evolution is combined with a constant movement through the ISM.

Mass loss via a stellar wind has been modelled as a spherically symmetric constant mass-loss rate $\dot{M}$ with constant velocity v. In the ISM wind the density and velocity are constant.

Typical estimates from the literature are used for the wind parameter values. The post-AGB fast wind parameters are: $\dot{M}_{\mathrm{fw}} = 5 \times 10^{-8}$ $M_\odot$ yr^{-1}, $v_{\mathrm{fw}} = 1000$ km s^{-1} & $T_{\mathrm{fw}} = 5 \times 10^4$ K. The AGB slow wind parameters are: $\dot{M}_{\mathrm{sw}} = 10^{-6}$ $M_\odot$ yr^{-1}, $v_{\mathrm{sw}} = 15$ km s^{-1} & $T_{\mathrm{sw}} = 10^4$ K. The switch between the AGB wind and the post-AGB wind is instantaneous and occurs after 10^5 years of AGB evolution, which is suffiently long to allow a stable structure to develop. In view of the still considerable uncertainties on the detailed properties and evolution of these winds, more

detailed temporal variations were not modelled. In reality, one may expect the AGB wind to show increasing mass-loss rates with time, whilst the post-AGB may increase in velocity over time. However, the current assumptions are found to be sufficient to reproduce the basic structure of the nebula. The ISM itself is assumed to be homogeneous with characteristics of a warm neutral medium, the main constituent of the observed ISM: $T_{\mathrm{ISM}} = 2500$ K & $n_{\mathrm{H}} = 1$ cm^{-3} (Burton 1988). The gas pressure in all three winds is calculated assuming an ideal gas equation of state.

4   RESULTS

Various speeds of movement have been considered from 0 km s^{-1} to 175 km s^{-1} in steps of 25 km s^{-1}. The results of all these models can be found in Wareing (2005). We present here only the case of 125 km s^{-1} which we find best fits the general morphology of Sh 2-188. For comparison with observations we have considered the locations of the brightened arc and its faint completing ring, the location of the candidate central star (33 per cent of the geometric radius upstream of the ring centre), and the location of the connecting tails downstream of the nebula.

4.1   Post-AGB structure and evolution

The left panel of Fig. 4 shows density on a slice through the computational domain at $(y = 100)$ 1,000 years into the post-AGB (PN) phase. During the PN phase the wind decreases in density and increases in velocity resulting in an adiabatic shock that forms the bright shell of the planetary nebula. Before this point, the nebula would have been inside the AGB wind bubble created by the AGB wind bow shock. At the depicted time, the nebula has expanded enough to be interacting with the AGB wind bow shock. Whilst the nebular shell has a constant temperature all the way round, the upstream part of the shell is now compressing the AGB wind bow shock and thus has a far higher density. Velocities in this higher density region range up to 20 km s^{-1}. The right panel of Fig. 4 is a synthetic image obtained by squaring the density and collapsing the datacube along the line of sight. This is a simple approximation and does not account for temperature or optical depth. The nebula appears to be brightened upstream where the higher densities are located. The downstream portion of the nebula ring is faint yet clear behind the bright arc with the tails connecting together further downstream.

Fig. 5 shows the state of the PN–ISM interaction 2,000 years into the PN phase. At this stage, the object is most reminiscent of Sh 2-188. The upstream arc is brightened, there is a faint completion of the nebular ring and the tails connect together downstream. Velocities in the upstream bright arc range from 20 to 70 km s^{-1}. Importantly, the central star is now displaced 10 per cent of the geometric radius upstream of the geometric centre. The IPHAS observations of Sh 2-188 reveal the central star to be approximately 33 per cent of the geometric radius upstream of the geometric centre. The faint connection of the ring downstream is the part of the nebula responsible for this displacement. As the PN shell expands, it is slowed upstream by interaction with the AGB wind shock whereas downstream, the PN shell

Figure 3. An artificial combination of Fig. 1 and Fig. 2 showing the detail in the bright arc and the faint structure (with some blurring to allow combination of the images). The different IPHAS bands are colour-coded (see text). The Hα image includes the continuum. The faint central star is indicated on the image between the markers.
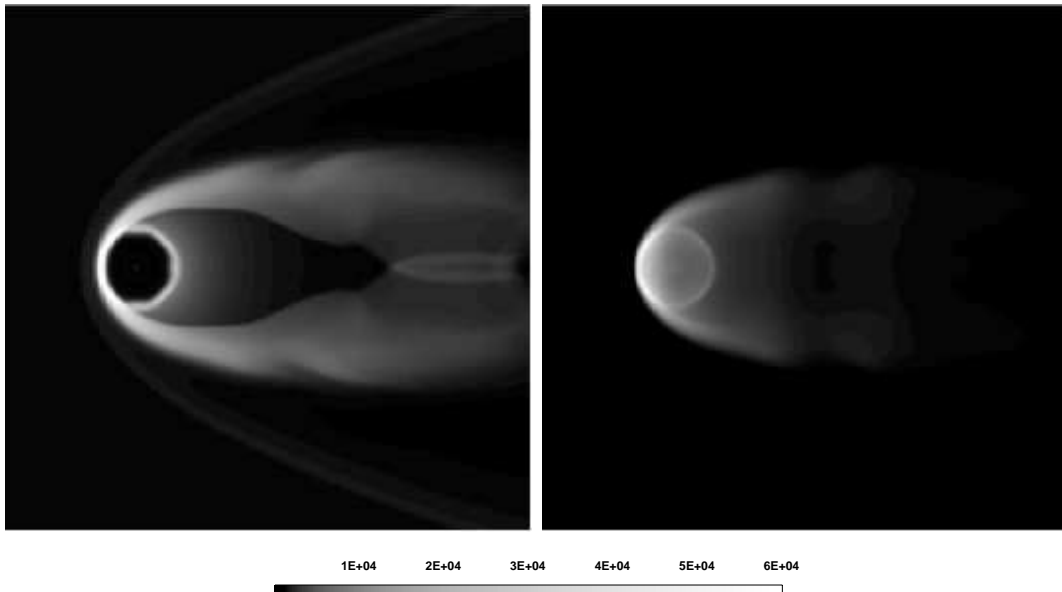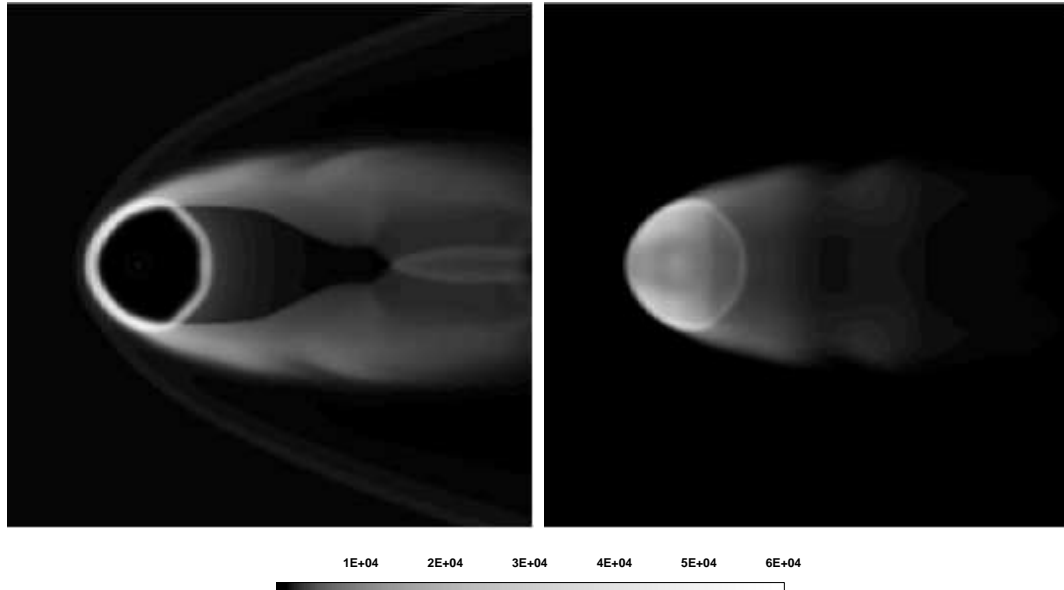

Figure 4. Shown on the left is a slice through the datacube showing the logarithm of density at a point 1,000 years into the PN phase. On the right is a representation of what the nebula might look like in emission. The images are 1 pc on a side. The scaling bar shown refers to the density slice and is presented in 10^{-6} $M_\odot$ pc^{-3}.
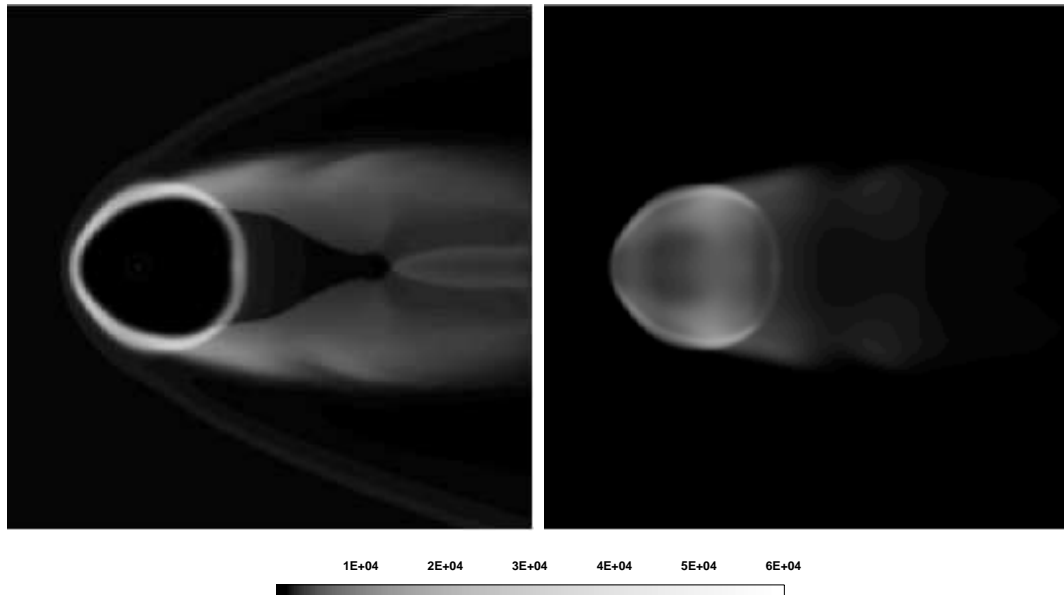
Figure 5. Shown on the left is a slice through the datacube showing the logarithm of density at a point 2,000 years into the PN phase. On the right is a representation of what the nebula might look like in emission. The images are 1 pc on a side. The scaling bar shown refers to the density slice and is presented in 10^{-6} M$_\odot$ pc^{-3}.

Figure 6. Shown on the left is a slice through the datacube showing the logarithm of density at a point 3,000 years into the PN phase. On the right is a representation of what the nebula might look like in emission. The images are 1 pc on a side. The scaling bar shown refers to the density slice and is presented in 10^{-6} M$_\odot$ pc^{-3}.

is progressing quicker through undisturbed AGB material, thus causing the geometric centre to move downstream.

The structure of the PN–ISM interaction after 3,000 years of the PN phase is shown in Fig. 6. The nebula is now departing from circular symmetry and hence appearing less like Sh 2-188. The brightest regions are moving downstream to where the PN shell is still interacting with the shocked AGB material in the tails. The velocities in these regions range between 20 and 50 km s^{-1} as do the velocities in the shocked high density material at the head of the bow shock.

The apparent displacement of the central star is approaching 30 per cent of the geometric radius, similar to the star in the case of Sh 2-188. Eventually, after the UV flux of the central star has turned off and the star has entered the white dwarf cooling regime, the fast wind will cease. At this time the whole nebula is swept downstream, and the star begins to desert its nebula as it continues to move at high speed, leaving its tail behind.
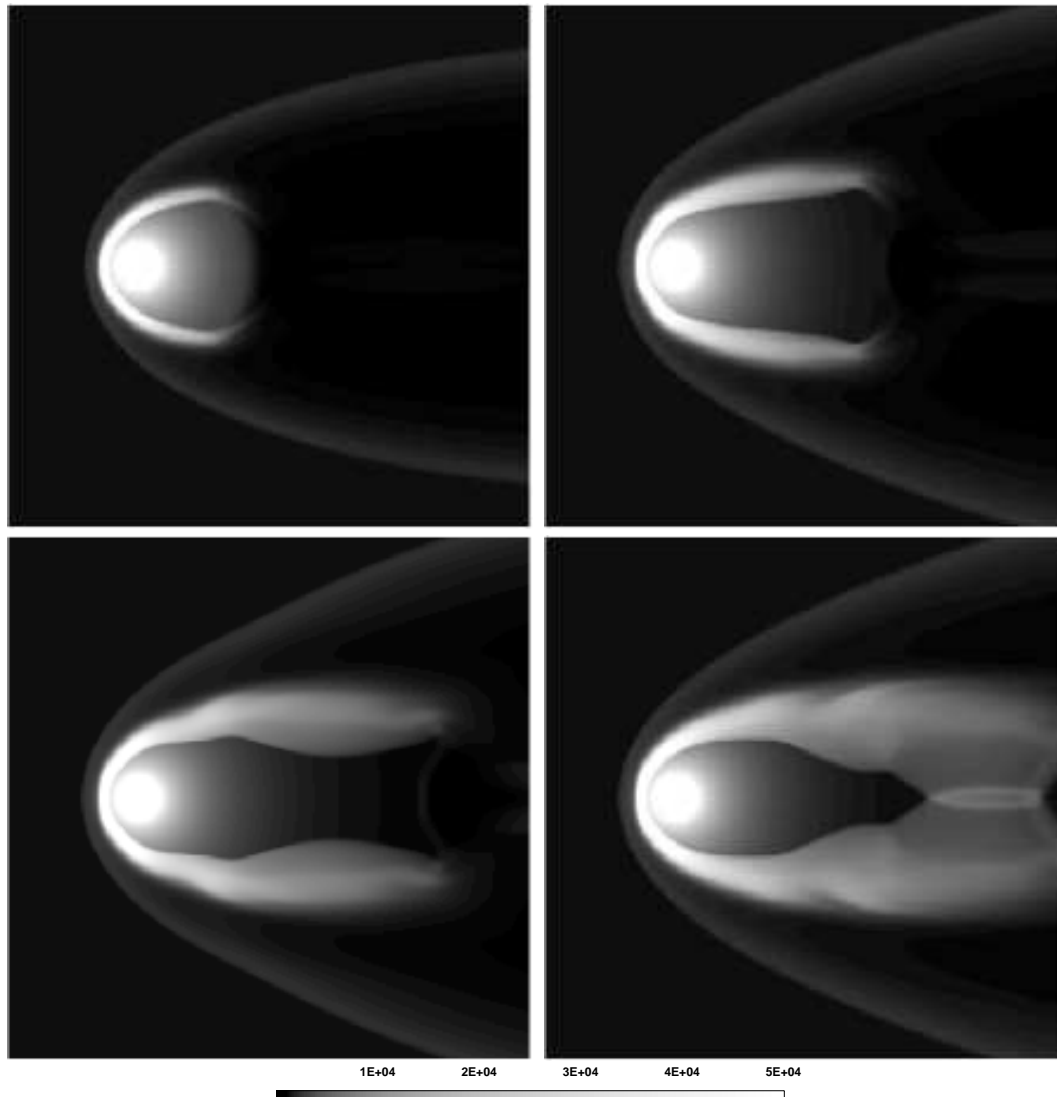
Figure 7. Logarithmic density plots showing the development of the bow shock structure and tails during the AGB phase of evolution for a central star with a peculiar velocity of 125 $\mathrm{km\,s^{-1}}$. The images are 1pc on a side. Panel A (upper left) is after 12,500 years, Panel B (upper right) after 25,000 years, Panel C (lower left) after 37,500 years and Panel D (lower right) after 50,000 years. Density is presented in 10^{-6} $\mathrm{M_\odot\,pc^{-3}}$.

4.2   AGB structure and evolution

The formation and evolution of the bow shock which so strongly influences the PN shaping is of interest. Fig. 7 shows a slice of the computational domain through the position of the central star at various times in the AGB phase. The panels illustrate the development of the bow shock and tail structure. Note that the true structure can be thought of as a rotation of the slices about the symmetry axis through the central star. Compression and deformation of the slow wind against the ISM rapidly forms a bow shock ahead of the star as shown in Panel A, 12,500 years after the start of the AGB phase. In Panel B, 25,000 years into the AGB phase, material stripped by ram pressure from the head of the bow shock is flowing downstream and beginning to form tails behind the nebula. Eventually, 37,500 years into the AGB phase, the flow collimates these tails downstream of the nebula and they appear to join. At this point in time

the structure has reached a stable state with the position of the reverse shock ahead of the central star being predicted by a simple ram-pressure-balance argument. The temperature of the shocked ISM material at the head of the bow shock is approximately 200,000 K. This is in agreement with strong shock theory which predicts the temperature to be $(3/16)\,(m\,v_{\mathrm{ISM}}^2/k)$, in this case a temperature of 205,500 K. Radiative cooling in the simulation has compressed this region. The shocked AGB material is ten times more dense and at a temperature of a few thousand K. The bow shock material cools as it is ram-pressure-stripped downstream. The structure shown in the fourth panel of Fig. 7 is the state after 50,000 years of the AGB phase, with material clearly flowing back down the tails. This structure does not change for the next 50,000 years. The injected stellar wind balances the material moving downstream.

An instability at the head of the bow shock causes ma-

terial to move down the tails in waves. This instability can be attributed to vortex shedding at the head of the bow shock, but the high flow velocity does not allow the vortices to form fully downstream. In our simulations of lower velocity central stars, this vortex shedding has been seen to destroy the smooth tail structure. This effect is not in the scope of this paper and will be discussed at length elsewhere.

4.3   Proper motion of the central star

Our simulation reproduces the observed features as described above, if the central star has a peculiar velocity of 125 km s^{-1}. If the star is within 1 kpc as predicted by various authors (see Table 1) and moving as we predict at 125 km s^{-1}, it should have an appreciable angular shift on the sky over a relatively short epoch. The heliocentric radial velocity is reported as $v_r = -26 \pm 10$ km s^{-1}. Corrections for the Solar motion and Galactic rotation approximately cancel. Thus, a tangential velocity $v_t = 122$ km s^{-1} with respect to the Local Standard of Rest (LSR) would be expected.

With this in mind, we have performed a proper motion analysis of the central star via astrometric methods. The observations used for this are detailed in Table 2. Initially we looked for a shift between the IPHAS observations discussed earlier and the observations of Tweedy & Kwitter (1996) taken in late 1992 at the 36 inch Burrell Schmidt telescope on Kitt Peak, using unbinned IPHAS images with a pixel size of $\frac{1}{3}$ arcsec. Tweedy and Kwitter's observations have a pixel size of 2.05 arcsec, which was insufficient to detect a shift in the position of the candidate central star.

Following this we found that the central star was listed in the USNO-B1 catalog (Monet et al. 2003) (star number 1484-0053964). This catalog obtained data from scans of 7,435 Schmidt plates taken for various sky surveys over the past 50 years. The candidate central star had been observed in 1976.9 to a high positional accuracy. We fitted the positions in the catalog to stars around the nebula up to a radius of 10 arcmin. The rms of the fit was 0.04 arcsec. We detected a significant shift of the candidate central star of 0.8 arcsec. This shift equates to a proper motion of the central star of Sh 2-188 of 26 ± 11 mas yr^{-1} in right ascension and of -15 ± 10 mas yr^{-1} in declination. The 1992.8 epoch position encompasses the expected position of the central star at that time.

This proper motion corresponds to a total displacement in the plane of the sky of 30 ± 10 mas yr^{-1}, with a position angle of $120° \pm 20°$ East through North. The proper motion corrections due to Galactic rotation and due to the Solar motion approximately cancel in this direction. Assuming the central star is moving at 122 ± 25 km s^{-1}, the distance to the nebula is estimated to be 850^{+500}_{-420} pc. This distance range is in good agreement with the estimates of Napiwotzki (1999, 2001) and Saurer (1995). The measured proper motion is in the direction expected from our simulation supporting the identification of the central star of Sh 2-188.

Although the agreement of our simulation with observation is encouraging, this should not be overstated. We have investigated a large parameter range in velocity, but the range of possible density contrasts is very large and we do not claim the final result is unique. In fact, now the distance has been determined, we can also compare the physical size of the nebula with the simulation: this reveals that the ini-

tial solution predicts a far smaller nebula than is observed. A solution to this discrepancy is discussed in the next section.

5   THE SIZE OF THE NEBULA

If, as the proper motion combined with the simulation predicts, the central star is at 850 pc, there is a discrepancy over the physical size of the nebula between the observations and simulation. The observations show the nebula is 2.5 pc in diameter whereas in the simulation it is only around one tenth of this size. The large difference requires a change to the assumed values of the physical parameters. Since the proper-motion distance and other distance determinations agree, we keep the velocities unchanged and adjust the densities. This approach is also suggested by the fact that observed AGB (super) wind velocities vary by not much more than a factor of 2, whilst the mass-loss rates can vary by a factor of 100. A similar argument can be made for the ISM density versus the peculiar velocity.

A simple rescaling of the simulation allows one to change the densities and radii, without changing the dimensionless model results. We wish to generalise the model holding the velocities in the simulation constant and increase the size of the nebula by a factor of ten. The size of the nebula is defined by the size of the AGB wind bubble which is in turn described by a simple ram pressure balance argument. To move the physical position of the ram-pressure balance point (reverse shock of the AGB wind bow shock) 10 times further upstream requires a factor of 100 increase from the ratio of slow-wind mass loss to ISM density, when keeping velocities constant. Increasing mass, length and time by a factor of ten decreases density by a factor of 100. Thus the simulation domain and nebula are ten times larger. The time scales also increase by a factor of 10: now 500,000 years on the AGB is required for a stable morphology to develop. This is in line with the 495,000 year AGB evolution predicted analytically by Vassiliadis & Wood (1993, 1994). The surrounding ISM has dropped in density from 1 cm^{-3} to 0.01 cm^{-3}, a value consistent with the warm ionised medium (WIM) rather than warm neutral medium. The rescaling shows that we do not in any way predict the mass-loss rate in the slow wind, only the ratio between the mass-loss rate and ISM density. The snapshots of the nebula and AGB evolution presented in the results section become 10 times older and Sh 2-188 now appears most like the simulation after 20 to 30,000 years of PN evolution. Thus, the distance, diameter and age are all in accordance with Napiwotzki (1999, 2001) and Saurer (1995).

Cooling times and cooling effects in the simulation are related to density and so decreasing the density by a factor of 100 alters the cooling. We have rerun the simulation with this rescaling and found that the altered cooling produces the same morphology as the initial simulation, thus the rescaling seems entirely reasonable.

6   DISCUSSION

The triple-wind model can reproduce the appearance of the nebula Sh 2-188. Accepting the model, the nebula has a peculiar motion with respect to the local ISM of 125

Table 2. A summary of observations of the central star of Sh 2-188 used in the estimation of proper motion. The Δ values give the measurement uncertainties. The IPHAS star has a magnitude of $r' = 17.4$ and $r' - H\alpha = r' - i' = 0.0$.

epoch	α hh mm ss.s	δ dd ′ ″	$\Delta\alpha$ ″	$\Delta\delta$ ″	Source
1976.9	01 30 33.113	58 24 50.680	0.128	0.094	USNO-B1 (Monet et al. 2003)
1992.8	01 30 33.185	58 24 49.540	1.0	1.0	Tweedy & Kwitter (1996)
2003.8	01 30 33.203	58 24 50.290	0.165	0.165	IPHAS r-band (Drew et al. 2005)

$km\,s^{-1}$. The peculiar motion is mostly in the plane of the sky with the radial velocity around -25 $km\,s^{-1}$. The star is located close to the Galactic plane suggesting the star belongs to the disk population. The average transverse motion of a PN-forming central star in the Galactic disk is 40-60 $km\,s^{-1}$ (Binney & Merrifield 1998; Dgani & Soker 1998; Skuljan et al. 1999). The tail of the distribution extends up to 130 $km\,s^{-1}$ (Skuljan et al. 1999; Feast & Whitelock 2000). The velocity of the central star is therefore high, yet not unfeasibly high. It would be less extreme if the star were a thick disk star which have local average velocities of $50-75$ $km\,s^{-1}$ (Binney & Merrifield 1998).

High peculiar velocities are more likely in older stellar populations. This is in conflict to the type-I classification of the nebula: the nitrogen enrichment indicates a more massive progenitor. However, the high [N II]/Hα ratio may be caused by shock excitation, and does not necessarily imply an N overabundance. Further evidence of shock excitation is provided by the observation that the sulphur lines are stronger than Hβ λ4861 lines at all points where they have been measured (Kwitter 1979).

The central star of Sh 2-188 belongs to the tail of the velocity distribution of (older) disk stars. Its rarity is borne out in the unique filamentary, one-sided appearance of the nebula, which is without parallel among known Galactic PNe. The simulations presented in Wareing (2005) show that a velocity of less than 75 $km\,s^{-1}$ does not result in connecting tails behind the nebula and between 50 and 100 $km\,s^{-1}$ vortex shedding from the head of the bow shock seems to destroy the smooth tail structure observed in the nebula. A speed in the region of 125 $km\,s^{-1}$ (using increments of 25 $km\,s^{-1}$) is thus the lowest speed from the simulations at which the morphology of Sh 2-188 is reproduced.

The observed fragmentation of the bow shock can be understood in terms of the effect predicted by Dgani & Soker (1994, 1998) (hereafter referred to as DS). They postulated that Rayleigh-Taylor instabilities would fragment a bow shock in the direction of motion. Magnetic fields would suppress certain modes of fragmentation and accentuate others, changing the appearance. Sh 2-188 is located in the Galactic plane and thus DS interpreted its fragmentation as being an effect of fluid and magnetic field instabilities. Importantly, DS conclude that fragmentation of a substantial part of the halo occurs only for a proper motion of greater than 100 $km\,s^{-1}$. This provides a lower limit to the proper motion of Sh 2-188 and supports the proper motion inferred from the simulation of 125 $km\,s^{-1}$. There is no fragmentation in the simulation which could be attributable to a lack of resolution, the lack of magnetic field or a lack of a gravitational field. Further, there is in reality temporal evolution of the

slow wind, with thermal pulses at the end of the phase. It is possible that these pulses of high mass-loss could stratify and fragment the bow shock structure before the PN phase. As long as the lifetime of these stratifications allows them to survive late into the PN phase (which is questionable), the fast wind could reveal and further fragment them in a similar manner to the observed filamentary structure.

Spectroscopic data of the bright filaments taken by Rosado & Kwitter (1982) revealed velocities between 20 and 70 $km\,s^{-1}$. The velocities in the simulation show the same range in the high density regions at the head of the bow shock which in reality is thought to have fragmented forming the observed filamentary structure. This agreement between the simulation and observations is very encouraging, although no more velocity data on this object are available to us for a more detailed comparison at this time. It should be noted that in our model these velocities are not related to the nebular expansion, but instead to the flow of shocked material from the head of the bow shock back down the tails.

The faint emission completing the bright arc is particularly important. In the simulation this structure has a transitory nature and moves quickly away from the central star: it traces the interaction between the fast post-AGB wind and the slow AGB wind (elsewhere in the nebula this front has merged with the ISM shock). One reason for the fast movement of this shock is the high ratio of post-AGB/AGB momentum which we use.

The distance downstream of the ring from the central star compared to the distance upstream of the bright arc defines the shift of the geometric centre and provides a calibrator for the simulation presented here. The rescaling of the simulation predicts the age of the nebula between 20 and 25,000 years. Napiwotzki (1999, 2001) suggests that the star is 22,000 years into the post-AGB phase.

The simulation is not entirely in agreement with the observations. The progressive displacement of a star from the geometric centre of a nebula is an indicator of evolution and in the case of large nebulae, advanced evolution (Tweedy & Kwitter 1996). The central star of Sh 2-188 appears to be approximately 33 per cent of the geometric radius towards the bright arc from the geometric centre. The rescaled simulation indicates that after 20,000 years of PN evolution, the star should appear 10 per cent of the geometric radius upstream of the geometric centre. 10,000 years later, the simulation shows the central star approaching 30 per cent of the geometric radius upstream, in better agreement with the observations. However, by this time, the simulation predicts the bright regions of emission will have begun to shift downstream to where the PN shell is interacting with the tail. A better representation of the time-dependent stel-

lar winds may be needed to resolve this issue. Napiwotzki (1999, 2001) locate the star near the start of the white dwarf cooling track. At this point, the wind is expected to cease. The forward ram shock will no longer be supported by internal pressure and will retreat. The nebula will be blown downstream and disintegrate, and the white dwarf will appear to move out of its nebula. This phase is not included in the simulation. However, it implies that the Sh 2-188 morphology has a limited life expectancy.

Interaction with the ISM considerably alters the amount of mass within the circumstellar envelope during the AGB and post-AGB phases. The simulation reaches a point of stability during the life time of the AGB evolution (Vassiliadis & Wood 1993, 1994): a longer AGB wind does not increase the mass of the shell. After 20,000 years of the PN phase, an investigation of the (rescaled) simulation reveals that $0.6 \ M_\odot$ has been introduced into the spherical region of the nebula. This is made up of $0.5 \ M_\odot$ lost by the star and $0.1 \ M_\odot$ of ISM material entering the cross section of the nebula. An integration of the datacube over a roughly spherical region centred on the central star with the nebular radius estimates $0.236 \ M_\odot$ remaining within the PN boundary. Thus, $0.364 \ M_\odot$ of material has been swept downstream into the tail of the nebula. In fact, the observed tail of the nebula is far older than the nebula itself as it is made up of AGB and ISM material swept downstream. It is likely that most of the ISM material introduced into the stellar region has been swept downstream, but still a minimum of $0.264 \ M_\odot$ of stellar material has been mixed with the ISM downstream providing an efficient method of returning stellar material directly to the ISM.

Observations have revealed a missing mass problem in PNe whereby only a small fraction of the mass ejected during the AGB phase is inferred to be present during the post-AGB phase. Stellar evolution calculations predict that stars with initial masses in the range of 1-5 $M_\odot$ will end as PN nuclei with masses around 0.6 $M_\odot$. Most of the mass is lost during the AGB phase and should be easily observable as ionised mass during the PN stage. However, observations of Galactic PNe have revealed on average only 0.2 $M_\odot$ of ionised gas. Several PNe have been shown to have embedded molecular clumps which could contain much of this missing mass and these clumps have shown to survive ablation by stellar winds and therefore could survive into the PN phase (Pittard et al. 2005). The stripping of mass downstream of a moving PNe as investigated here also provides an attractive solution to this missing mass problem; the Dumbbell nebula appears to have clumps of material surrounding the bright nebula inside what would appear to be an AGB wind bow shock (Meaburn et al. 2005) combining both of these solutions to the missing mass problem.

Observations (Napiwotzki 1999, 2001) have indicated that the central star of Sh 2-188 has a mass of 0.6 $M_\odot$. These observations, in combination with the mass injected into our simulation and the addition of mass lost prior to the superwind phase (a typical estimate for low-mass stars being $\lesssim 0.5 \ M_\odot$) allows us to estimate a mass of $\sim 1.5 \ M_\odot$ for the progenitor star.

Villaver et al. (2002) discussed evolution of AGB stars and the interaction of their dust shells with the ISM. Typically, AGB stars form large shells (up to 4 pc in diameter) around them. Evidence for such an AGB–ISM interaction

front was found by Zijlstra & Weinberger (2002), who found a M3 III AGB star surrounded by such a detached shell of 4 pc diameter. The ISM influence is defined by the density and hence pressure in the ISM, which drops off exponentially from $n_H = 2 \ cm^{-3}$ (Spitzer 1978) at a scale height of 100 pc (Binney & Merrifield 1998). The regular shells can be influenced strongly by the movement through the surrounding ISM. The AGB evolution of the central star of Sh 2-188 shows a structure extensively altered from these regular dust shells. Much of the AGB material has been swept downstream.

At a distance of 850 pc, the nebula is 60 pc below the Galactic plane. We would expect the ISM density in the region of Sh 2-188 to be around $n_H = 2 \ cm^{-3}$ so it would seem our rescaling choice of $n_H = 0.01 \ cm^{-3}$ is at odds with this. However, large regions of the Galactic plane in between spiral arms are dominated by such low-density gas, including the volume around the Sun (Frisch 1995). In fact, the NE2001 model (Cordes & Lazio 2002), used commonly in the Pulsar community to predict the galactic distribution of free electrons, predicts an electron density in the direction of Sh 2-188 of $n_e = 0.013 \ cm^{-3}$ at a distance of 850 pc. This is in very good agreement with our prediction, but it should be stressed that this is only one choice of AGB mass-loss rate to ISM density ratio. A higher mass-loss rate would increase the ISM density, although this would have implications for the mass in the nebular region. The direction of motion indicates the star is moving almost entirely in Galactic longitude and has travelled 64 pc during the AGB and post-AGB phases. Therefore the assumption of constant ISM properties during the AGB and post-AGB evolution of the central star may not be correct.

7 CONCLUSIONS

We have successfully reproduced the morphology and the available kinematic data of Sh 2-188 and understood its formation in terms of the 'triple wind' model. Following the AGB evolution of the central star has been crucial in fitting the whole structure, in particular the tail behind the nebula which is comprised of purely AGB material. The triple-wind model of Sh 2-188 has predicted a velocity of the candidate central star of 125 km s^{-1}. Velocities from spectroscopic data on the bright filaments (Rosado & Kwitter 1982) are in agreement with velocities measured from the simulation. A proper motion study of the central star has shown it to be moving at 30.0 ± 10.0 mas yr^{-1} in the direction of the head of the bright arc. The combination of these two measurements has resulted in estimates of $D = 850^{+500}_{-420}$ pc, $d \sim 2.5$ pc and $t_{PN} = 22,500 \pm 2,500$ years. These estimates are in agreement with the distance and age estimates of Saurer (1995) and Napiwotzki (1999, 2001). The prediction of ISM density in the vicinity of Sh 2-188 is also in agreement with the NE2001 model of Cordes & Lazio (2002). The triple wind model explains the geometric displacement of the central star and indicates that the faint closure of the bright arc is a transitory structure which evolves downstream of the nebula. The PN–ISM interaction has caused $\approx \frac{2}{3}$ of the mass expected in the region of the star to be swept downstream providing a solution to the missing mass phenomenon in PN

and a valuable way of mixing ISM and stellar material several pc downstream of the central star.

The success of the triple-wind model to fit this extreme object gives confidence in our ability to fit objects with lower speeds. It is now clear that the outer halo structure of PNe contain the effects of ISM interaction and should not be modelled as stand-alone structures. Further, the ISM interaction is an important method of mixing stellar material back into the ISM. The next generation of telescopes, particularly ALMA, will be able to reveal cool dust structure in the universe and shed light on circumstellar AGB material. Further simulations considering temporal evolution of the stellar winds, magnetic fields and/or gravity may shed light on why we have not reproduced the observed fragmentation in Sh 2-188.

REFERENCES

Acker A., Marcout J., Ochsenbein F., Stenholm B., Tylenda R., 1992, Strasbourg - ESO catalogue of galactic planetary nebulae (Garching: European Southern Observatory)
Balick B., 1987, AJ, 94, 671
Binney J., Merrifield M., 1998, in Galactic Astronomy (Princeton, NJ: Princeton University Press), Ch. 10
Borkowski K.J., Sarazin C.L., Soker N., 1990, ApJ, 360, 173
Burton W.B., 1988, in Galactic and Extragalactic Radio Astronomy, ed. K. Kellermann & G.L. Verschuur (New York: Springer), 295
Cahn J.H., Kaler J.B., Stanghellini L., 1992, A&AS, 94, 399
Cordes J.M., Lazio T.J.W., 2002, preprint (astro-ph/0207156)
Dgani R., Soker N., 1994, ApJ, 434, 262

Dgani R., Soker N., 1998, ApJ, 495, 337
Drew J.E. et al., 2005, MNRAS, 362, 753
Falle S.A.E.G., 1991, MNRAS, 250, 581
Feast M.W., Whitelock P.A., 2000, MNRAS, 317, 460
Frisch P.C, 1995, Space Science Reviews, 72, 499
Gaze V.F., Shain G.A., 1965, Izv. Krym. Astrofiz. Obs., 15, 11
Gurzadyan G.A., 1969, Planetary Nebula (New York: Gordon & Breach), p.235
Isaacmann R., 1979, A&A, 77, 327
Israel F.P., Felli M., 1976, Pub. A.S.P., 87, 89
Johnson H.M., 1975, Pub. A.S.P., 87, 89
Kwitter K.B., 1979, PhD thesis, UCLA
Kwitter K.B., Jacoby G.H., Lydon T.J., 1988, AJ, 96, 997
Kwok S., 1982, AJ, 258, 280
Lozinskaya T.A., Esipov V.F., 1971, Soviet Astr.-AJ, 15, 353
Meaburn J. et al., 2005, Rev. Mex. AA, 41, 109
Monet D.G. et al., 2003, AJ, 125, 984
Napiwotzki R., Schoenberner D., 1995, A&A, 301, 545
Napiwotzki R., 1999, A&A, 350, 101
Napiwotzki R., 2001, A&A, 367, 973
Oort J.H., 1951, Problems of Cosmical Aerodynamics (Dayton: Central Air Document Office)
Parker R.A.R., 1964, ApJ, 139, 493
Peimbert M., 1981 in Physical Processes in Red Giants, p.409 (Dordrecht: D. Reidel)
Pittard J.M. et al., 2005, MNRAS, 361, 1077
Rosado M., Kwitter K.B., 1982, RevMexAA, 5, 217
Salter C.J., Greve A., Weiler K.W., Birkle K., Dennefeld M., 1984, A&A, 137, 291
Saurer W., 1995, A&A, 297, 261
Sharpless S., 1959, ApJS, 4, 257
Skuljan J., Hearnshaw J.B., Cottrell P.L., 1999, MNRAS, 308, 731
Smith H., 1976, MNRAS, 175, 419
Soker N., Borkowski K.J., Sarazin C.L., 1991, AJ, 102, 1381
Spitzer L. Jr, 1978, Physical Processes in the Interstellar Medium (New York: Wiley), p. 234
Tweedy R.W., Kwitter K.B., 1996, ApJS, 107, 255
Vassiliadis E., Wood P., 1993, ApJ, 413, 641
Vassiliadis E., Wood P., 1994, ApJS, 92, 125
Villaver E., Garcia-Segura G., Manchado A., 2002, ApJ, 571, 880
Villaver E., Garcia-Segura G., Manchado A., 2003, ApJL, 585, L53
Wareing C.J. 2005, PhD thesis, Univ. of Manchester, 2005
Zijlstra A.A., Weinberger R., 2002, ApJ, 572, 1006